Emerging Hawking-Like Radiation from Gravitational Bremsstrahlung Beyond the Planck Scale

Marcello Ciafaloni* and Dimitri Colferai†
Dipartimento di Fisica, Università di Firenze and INFN, Sezione di Firenze, Via Sansone 1, 50019 Sesto Fiorentino, Italy

Gabriele Veneziano‡
Collège de France, 11 place M. Berthelot, 75005 Paris, France and Theory Division, CERN, CH-1211 Geneva 23, Switzerland

(Received 12 June 2015; published 23 October 2015)

We argue that, as a consequence of the graviton's spin-2, its bremsstrahlung in trans-Planckian-energy ($E \gg M_P$) gravitational scattering at small deflection angle can be nicely expressed in terms of helicity-transformation phases and their transfer within the scattering process. The resulting spectrum exhibits deeply sub-Planckian characteristic energies of order $M_P^2/E \ll M_P$ (reminiscent of Hawking radiation), a suppressed fragmentation region, and a reduced rapidity plateau, in broad agreement with recent classical estimates.

DOI: 10.1103/PhysRevLett.115.171301 PACS numbers: 04.60.Bc, 04.30.Db, 04.70.Dy

It is well known that much—if not all—of the geometric beauty of classical general relativity can follow from assuming the existence, at the quantum level, of a massless spin-2 particle, the graviton. This is how we understand, for instance, that quantum string theory in flat space-time becomes a theory of quantum (and, in some approximation, of classical) gravity, though not necessarily Einstein's.

The emergence of a Schwarzschild metric through a resummation of graviton-exchange diagrams was pointed out long ago by Duff [1]. Much later, a similar approach was taken up in the context of string theory [2–6], where scattering at trans-Planckian energy ($E \gg M_P \equiv \sqrt{\hbar/G}$, in $c = 1$ units) was taken as the thought experiment of choice for understanding quantum string gravity as well as its quantum field theory and classical limits. It was possible to show [2] how an effective Aichelburg-Sexl metric [7] emerges, manifesting itself at a large-impact parameter ($b \gg R \equiv 4GE$) via the gravitational deflection and tidal excitation [2,8] of the incoming strings.

As one proceeds to smaller impact parameters, corrections of relative order R^2/b^2 appear [9,10]. These modify, of course, deflection angles and time delays [11–13], but also introduce as a new phenomenon graviton bremsstrahlung. At lowest order all of this can be studied in terms of the so-called H diagram [9,10], but its extension to higher orders turned out to be nontrivial. In particular, the most naive resummation appears to endanger energy conservation [14].

The purpose of this Letter is to go beyond the analysis of Refs. [9,10] and to show that the graviton's spin-2, besides making it possible for an effective metric to emerge, also determines the detailed form of graviton bremsstrahlung in a whole frequency and angular range, covering, in particular, the forward fragmentation regions responsible for the excessive energy emission. As we will show, taking properly into account coherence effects not only solves the energy-conservation issue, but also leads to a graviton's spectrum with characteristic energies of order $\hbar R^{-1}$, the typical energy of Hawking's radiation out of a black hole of mass E. The main features of such a picture are consistent with their classical counterparts recently discussed in Refs. [15,16]. In this Letter, we will sketch the derivation and present the main physical results leaving most of the technical details to a forthcoming paper [17].

In order to set the framework, consider first the elastic gravitational scattering $p_1 + p_2 \to p_1' + p_2'$ of two fast particles, at center-of-mass energy $2E = \sqrt{s} \gg M_P$, and momentum transfer Q^μ with transverse component $\boldsymbol{Q} \equiv E\boldsymbol{\Theta}_s$, where the 2-vector $\boldsymbol{\Theta}_s = |\boldsymbol{\Theta}_s|(\cos\phi_s, \sin\phi_s)$ describes both the azimuth ϕ_s and the polar angle $|\boldsymbol{\Theta}_s| \ll 1$ of the final particles with respect to the longitudinal z axis. This elastic scattering is described by the semi-classical S matrix, $\exp(2i\delta)$, whose leading term is given by the eikonal function $\delta_0 = (Gs/\hbar)\log(L/|\boldsymbol{b}|)$ (L being an irrelevant infrared cutoff). Its exponentiation describes the amplitude at impact parameter $\boldsymbol{b}$, conjugated to $\boldsymbol{Q}$, as a sum over a large number $\langle n\rangle \sim Gs/\hbar$ of single-hit processes provided by single-graviton exchanges of momenta $\boldsymbol{q}_j = E\boldsymbol{\theta}_j$ ($j = 1, \ldots, n$). The single-hit scattering angle is very small, of order $\theta_m \equiv \hbar/Eb$, while the overall scattering angle—though small for $b \gg R$—is much larger, of order $2(Gs/\hbar)\theta_m \simeq 2R/b$, the Einstein deflection angle.

In order to compute the emission amplitude of a graviton of momentum $q^\mu = \hbar\omega(1, \boldsymbol{\theta}, \sqrt{1-\boldsymbol{\theta}^2})$, we start by considering the single-exchange scattering amplitude of momentum transfer $\boldsymbol{q}_s = E\boldsymbol{\theta}_s$ ($\theta_s \sim \hbar/Eb \equiv \theta_m$) and discuss various angular regimes, under the assumption that the emitted graviton energy $\hbar\omega \ll E$. That restriction still allows for a huge graviton phase space, in which classical frequencies of order R^{-1}—and even much larger ones—are available, due to the large gravitational charge $\alpha_G \equiv Gs/\hbar \gg 1$. We will distinguish three regimes.

(a) $|\boldsymbol{\theta}_s| > |\boldsymbol{\theta}|$. In this regime, characterized by small emission angles and subenergies, the emission amplitude is well described by external-line insertions corresponding to the Weinberg current, but the collinear limit has no singularities because of helicity-conservation zeros.

(b) $|\boldsymbol{\theta}| > |\boldsymbol{\theta}_s| > (\hbar\omega/E)|\boldsymbol{\theta}|$. In this regime the subenergies reach the threshold of high-energy Regge behavior, still remaining in the validity region of external-line insertions, due to the condition $|\boldsymbol{q}_s| > |\boldsymbol{q}|$, which suppresses the emission from the exchanged-graviton line.

(c) Finally, in the regime $|\boldsymbol{\theta}_s| < (\hbar\omega/E)|\boldsymbol{\theta}|$ ($|\boldsymbol{q}_s| < |\boldsymbol{q}|$) the soft approximation breaks down, in favor of the high-energy amplitude [9], which also contains emission from the exchanged-graviton line [18].

In the "soft" regime (a) the amplitude is described by the Weinberg current [19] [$\eta_i = 1(-1)$ for incoming (outgoing) lines],

$$M_{\text{soft}}(E, \boldsymbol{Q}; q^\mu) = M_{\text{el}} J_W^{\mu\nu} \epsilon_{\mu\nu} \equiv M_{\text{el}} \frac{J_W}{\sqrt{2}},$$
$$J_W^{\mu\nu} = \kappa \sum_i \eta_i \frac{p_i^\mu p_i^\nu}{p_i \cdot q}, \quad \kappa \equiv \sqrt{8\pi G}, \tag{1}$$

where the complex polarization $\epsilon^{\mu\nu}$ (together with its complex conjugate) represents gravitons of definite helicity ∓ 2. More explicitly, we write $\epsilon^{\mu\nu} = (\epsilon^{\mu\nu}_{TT} + i\epsilon^{\mu\nu}_{LT})/\sqrt{2}$, where we conveniently fix the gauge by taking

$$\epsilon^{\mu\nu}_{TT} = \frac{\epsilon^\mu_T \epsilon^\nu_T - \epsilon^\mu_L \epsilon^\nu_L}{\sqrt{2}}, \qquad \epsilon^{\mu\nu}_{LT} = \frac{\epsilon^\mu_L \epsilon^\nu_T + \epsilon^\mu_T \epsilon^\nu_L}{\sqrt{2}},$$
$$\epsilon^\mu_T \equiv \left(0, -\varepsilon_{ij}\frac{q_j}{|\boldsymbol{q}|}, 0\right), \qquad \epsilon^\mu_L \equiv \frac{(q^3, \boldsymbol{0}, q^0)}{|\boldsymbol{q}|} - (+)\frac{q^\mu}{|\boldsymbol{q}|}, \tag{2}$$

for q nearly parallel to p_1, p_1' (p_2, p_2'). Concentrating on the former case, a simple calculation gives

$$\frac{J_W}{\sqrt{2}} = \frac{\kappa E}{\hbar\omega} e^{-2i\phi_\theta}\left(e^{2i\phi_{\theta-\Theta_i-\theta_s}} - e^{2i\phi_{\theta-\Theta_i}}\right). \tag{3}$$

Multiplying now Eq. (3) by the elastic amplitude, we get the following b-space emission amplitude,

$$\mathcal{M}_{\text{soft}}(\boldsymbol{b}, E; \omega, \boldsymbol{\theta}) = \sqrt{\frac{Gs}{\hbar}} \frac{R}{\pi} \frac{E}{\hbar\omega} \times \int \frac{d^2\boldsymbol{\theta}_s}{2\pi\boldsymbol{\theta}_s^2} e^{i(E/\hbar)\boldsymbol{b}\cdot\boldsymbol{\theta}_s} e^{-2i\phi_\theta} \times \frac{1}{2}\left(e^{2i\phi_{\theta-\theta_s}} - e^{2i\phi_\theta}\right), \tag{4}$$

together with its transformation under change in the incidence angle $\boldsymbol{\Theta}_i$,

$$\mathcal{M}^{(\boldsymbol{\Theta}_i)}_{\text{soft}} = e^{2i(\phi_{\theta-\Theta_i} - \phi_\theta)} \mathcal{M}_{\text{soft}}(\boldsymbol{b}, E; \omega, \boldsymbol{\theta} - \boldsymbol{\Theta}_i). \tag{5}$$

Several remarks are in order. First, the current projection shows the expected $1/\omega$ dependence, but no singularities at either $\boldsymbol{\theta} = \boldsymbol{\Theta}_i$ or $\boldsymbol{\theta} = \boldsymbol{\Theta}_f = \boldsymbol{\Theta}_i + \boldsymbol{\theta}_s$, as we might have expected from the $p_i \cdot q$ denominators in Eq. (1). This is due to the spin-2 of the graviton, with the physical projections of the tensor numerators in Eq. (1) providing the result in terms of scale-invariant phases with azimuthal dependence. Second, Eq. (5) shows a simple dependence on the incidence angle $\boldsymbol{\Theta}_i$, which is interpreted as the helicity-transformation phase in turning the direction $\boldsymbol{\Theta}_i$ onto the $\vec{z}$ axis in 3-space, rotation in which the lightlike vector $q^\mu(\boldsymbol{\theta})$ undergoes the small-angle translation $\boldsymbol{\theta} \to \boldsymbol{\theta} - \boldsymbol{\Theta}_i$. Finally, the helicity phase transfer in Eq. (3) can be interpreted by the z representation [$z \equiv x + iy$, $\boldsymbol{z} \equiv (x, y)$],

$$e^{2i\phi_{\theta_A}} - e^{2i\phi_{\theta_B}} = \int \frac{d^2 z}{\pi z^{*2}} \left(e^{i\omega \boldsymbol{z}\cdot\boldsymbol{\theta}_B} - e^{i\omega \boldsymbol{z}\cdot\boldsymbol{\theta}_A}\right), \tag{6}$$

as an integral between initial and final directions in the transverse $\boldsymbol{z}$ plane of the complex component of the Riemann tensor [15] in the Aichelburg-Sexl metric of the incident particles.

If we now move to larger angles $\theta > \theta_m$, the subenergies increase and Regge behavior, as described by the Lipatov current [18] (see also Ref. [9]),

$$\frac{J_L^{\mu\nu}}{\boldsymbol{q}_{\perp 1}^2 \boldsymbol{q}_{\perp 2}^2} \equiv \frac{\kappa}{2}\left(\frac{J^\mu J^\nu}{\boldsymbol{q}_{\perp 1}^2 \boldsymbol{q}_{\perp 2}^2} - j^\mu j^\nu\right), \qquad j^\mu \equiv \frac{p_1^\mu}{p_1 q} - \frac{p_2^\mu}{p_2 q},$$
$$J^\mu \equiv \boldsymbol{q}_{\perp 1}^2 \frac{p_1^\mu}{p_1 \cdot q} - \boldsymbol{q}_{\perp 2}^2 \frac{p_2^\mu}{p_2 \cdot q} + q_1^\mu - q_2^\mu - \boldsymbol{q}_\perp^2 j^\mu \tag{7}$$

(here the $\boldsymbol{q}_\perp$'s are transverse to the $\vec{p}_1$ direction), is turned on. By performing the same projection as before, we get the Regge counterpart of Eqs. (4) and (5):

$$\mathcal{M}_{\text{Regge}}(\boldsymbol{b}, E; \omega, \boldsymbol{\theta}) = \sqrt{\frac{Gs}{\hbar}} \frac{R}{\pi} \times \int \frac{d^2\boldsymbol{q}_2}{2\pi\boldsymbol{q}^2} e^{i(\boldsymbol{q}_2\cdot\boldsymbol{b}/\hbar)} \times \frac{1}{2}\left(1 - e^{-2i(\phi_{q_2} - \phi_{q_2 - q})}\right),$$
$$\mathcal{M}^{(\boldsymbol{\Theta}_i)}_{\text{Regge}} = e^{2i(\phi_{\theta-\Theta_i} - \phi_\theta)} \mathcal{M}_{\text{Regge}}(\boldsymbol{b}, E; \omega, \boldsymbol{\theta} - \boldsymbol{\Theta}_i), \tag{8}$$

with the same transformation law as before. Note that a helicity phase transfer occurs also in Eq. (8), except that the transfer is now in the t (rather than in the s) channel (Fig. 1).

Equation (8) has an explicit representation in terms of $\tilde{h}(\boldsymbol{b}, \boldsymbol{q})$, the radiative metric field [10], and of its $\boldsymbol{x}$-space Fourier transform counterpart $h(\boldsymbol{b}, \boldsymbol{z})$,

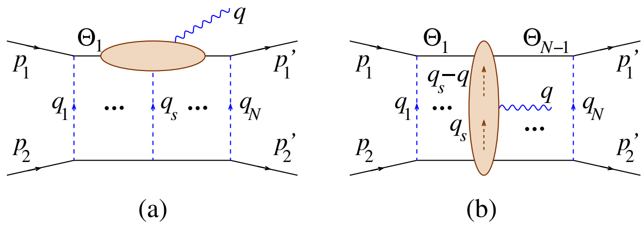

FIG. 1 (color online). Picture and notation of generic exchange emission in (a) the soft and (b) the Regge limits. Here, $\boldsymbol{q}_s = \boldsymbol{q}_2$ for the single-exchange amplitude [Eq. (8)].

$$\mathcal{M}_{\text{Regge}} = \sqrt{\frac{Gs}{\hbar}}\frac{R}{2}\tilde{h}(\boldsymbol{b},\boldsymbol{q}),$$
$$h(\boldsymbol{b},z) = \frac{1-e^{2i(\phi_z-\phi_{z-b})}}{2\pi^2 b^2} = \frac{iy}{\pi^2 b z^*(z-b)}, \quad (9)$$

as found in part in Ref. [10] and proved in Ref. [17].

Our main observation now is that soft and Regge evaluations agree in the (b) region. In fact, by setting $\boldsymbol{q}_2 = \boldsymbol{q}_s = E\boldsymbol{\theta}_s$ and $\boldsymbol{q} = \hbar\omega\boldsymbol{\theta}$, we can compute the difference (in complex-θ notation):

$$\mathcal{M}_{\text{Regge}} - \mathcal{M}_{\text{soft}} = \sqrt{\frac{Gs}{\hbar}}\frac{R}{2\pi}\frac{E}{\hbar\omega}\int\frac{d^2\theta_s}{2\pi|\theta_s|^2} \times\frac{\theta\theta_s^*-\theta^*\theta_s}{|\theta|^2}e^{i(E/\hbar)\boldsymbol{b}\cdot\boldsymbol{\theta}_s}\left[\frac{1}{1-\frac{\hbar\omega}{E}\frac{\theta^*}{\theta_s^*}}-\frac{1}{1-\frac{\theta_s^*}{\theta^*}}\right], \quad (10)$$

which is clearly vanishing in the angular region $|\theta| \gg |\theta_s| \gg (\hbar\omega/E)|\theta|$. This ensures the large-angle regime for the soft amplitude with negligible internal insertions in the Regge amplitude. Furthermore, Eq. (10) can be used to replace the soft amplitude with the Regge one in region (c) in which the former breaks down. Since that is a large-angle region, the last term can be replaced by -1 and—with this proviso—a rescaling of angles in which $\tilde{\theta}_s \equiv (E\theta_s/\hbar\omega)$ is fixed shows that in region (c) Eq. (10) is just the negative of $\mathcal{M}_{\text{soft}}$ at $E = \hbar\omega$.

In conclusion, our matched amplitude, at the single-exchange level, is

$$\mathcal{M} \equiv \mathcal{M}_{\text{soft}}(\boldsymbol{b},E;\omega,\theta) - \mathcal{M}_{\text{soft}}(\boldsymbol{b},\hbar\omega;\omega,\theta)$$
$$\simeq -R\sqrt{\frac{Gs}{\hbar}}\frac{e^{-2i\phi_\theta}}{2\pi^2}\int\frac{d^2z}{z^{*2}}e^{ib\omega z\cdot\boldsymbol{\theta}}\Phi(z),$$
$$\Phi(z) \equiv \hat{\boldsymbol{b}}\cdot z + \log|\hat{\boldsymbol{b}} - z|, \quad (11)$$

where the expression on the second line, valid in the $\theta > \theta_m$ region, is obtained in a straightforward way [17] by using the z representation [Eq. (6)] in the definition [Eq. (4)] of the soft amplitude.

We shall call Eq. (11) [Eq. (9)] the soft-based [Regge-based] representation of the same unified amplitude. Their identity can be shown [17] to be due to a transversality condition of the radiative metric tensor [10] and is thus rooted in the spin-2 nature of the interaction.

Our next step is to extend the above procedure to any active exchanges in the eikonal chain, and to resum them, by taking into account two important facts: (i) the amplitude transformation [Eqs. (5) and (8)] with incidence angle $\boldsymbol{\Theta}_i$—possibly much larger that θ_m, and (ii) the nontrivial extension of b-space factorization to any incidence angle. The matter is discussed in detail in the parallel paper [17], but the final answer is easy to understand. The resummed single-emission soft-Regge amplitude, factorized in front of the elastic eikonal S matrix, is

$$\mathfrak{M} \equiv \frac{\mathcal{M}}{e^{2i\delta}} = \int_0^1 d\xi\mathcal{M}_{\text{Regge}}^{(\xi\boldsymbol{\theta}_s)} = \sqrt{\frac{Gs}{\hbar}}\frac{R}{2} \times\int_0^1 d\xi e^{2i(\phi_{\theta-\xi\theta_s}-\phi_\theta)}\int d^2z e^{ib\omega z\cdot(\boldsymbol{\theta}-\xi\boldsymbol{\theta}_s)}h(\boldsymbol{b},z). \quad (12)$$

It represents the coherent average of the single-exchange result of Regge type at incidence angle $\xi\boldsymbol{\theta}_s$ ranging from 0 to $\boldsymbol{\theta}_s(\boldsymbol{b}) \equiv (2R/b)\hat{\boldsymbol{b}}$, with the corresponding transformation phase. This is even more transparent in an alternative equivalent expression incorporating the transformation phase

$$\frac{-\mathfrak{M}}{e^{-2i\phi_\theta}} = \sqrt{\frac{Gs}{\hbar}}\frac{R}{\pi}\int_0^1 d\xi\int\frac{d^2z}{2\pi z^{*2}}e^{ib\omega z\cdot(\boldsymbol{\theta}-\xi\boldsymbol{\theta}_s)}\Phi(z), \quad (13)$$

in which the soft-based form [Eq. (11)] in terms of $\Phi(z)$ is used. The final result [Eq. (13)] compares easily with the classical result of Ref. [15]: it is the ξ average of the classical amplitude, expanded to first order in the modulation factor $\Phi(z)$.

Our last step consists in using b factorization to resum multigraviton emission, at least for the independent pairs, triples, etc. of active exchanges that dominate by combinatorics at high energy. Because of the exponential counting in eikonal scattering, this provides for us the so-called linear coherent-state operator in the form

$$\frac{\hat{S}}{e^{2i\delta}} = \exp\int\frac{d^3\vec{q}}{\sqrt{2\omega}}2i\left[\sum_{\lambda=\pm}\mathfrak{M}_{\boldsymbol{b}}^{(\lambda)}a_{(\lambda)}^\dagger(\vec{q}) + \text{H.c.}\right], \quad (14)$$

where the helicity amplitude $\mathfrak{M}_{\boldsymbol{b}}^{(-)}(\vec{q}) = [\mathfrak{M}_{\boldsymbol{b}}^{(+)}(q_3,-\boldsymbol{q})]^*$ is provided by Eq. (13) with a proper identification of variables. Since operators associated with opposite helicities commute, the above coherent state is Abelian (and thus consistent with the Block-Nordsieck theorem), but describes both helicities, not only the infrared singular, longitudinal polarization.

We are finally ready to discuss the gravitational-wave (GW) spectrum. By normal ordering in the coherent state [Eq. (14)], we obtain the energy-emission distribution

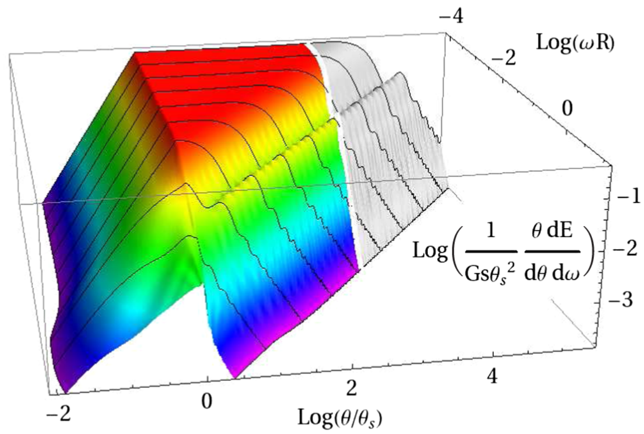

FIG. 2 (color online). Azimuthally integrated spectrum versus ωR and θ/θ_s. The shaded region on the right is excluded by the kinematic bound $\theta < 1$ (for the choice $\theta_s = 10^{-3}$).

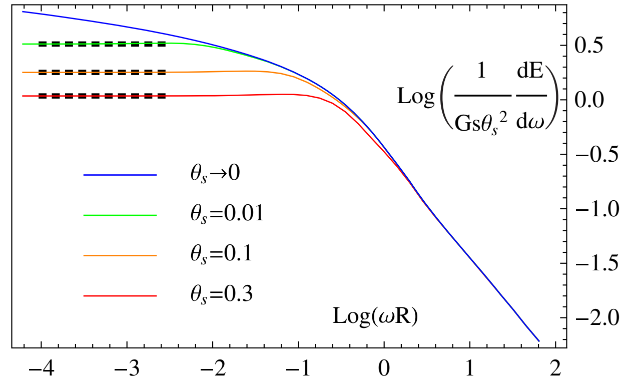

FIG. 3 (color online). Frequency spectrum of gravitational radiation for various values of θ_s. For each θ_s the ZFL value $(2/\pi)\log(1.65/\theta_s)$ is obtained (dashed lines).

$$\frac{dE^{\mathrm{GW}}}{d\omega d\cos\theta d\phi} = \omega^2 \hbar 2 \sum_\lambda |\mathfrak{M}_{\boldsymbol{b}}^{(\lambda)}|^2. \tag{15}$$

The main features of the spectrum can be understood analytically, but can be best described following the numerical results presented in Fig. 2 (where we have integrated over the azimuthal angle ϕ) and Fig. 3 (where we have also integrated over the polar angle $|\theta|$).

Figure 2 shows very clearly that the spectrum is dominated by a flat plateau (where kinematically accessible) whose shape can be easily explained as follows. The spectrum falls on the left ($\theta < \theta_s$) because of phase space and the absence of collinear singularities. It also falls when $\omega R = bq\theta_s/\theta > \theta_s/\theta$, since then $bq > 1$. The last limitation (shaded region on the right) is due to the trivial kinematic bound $\theta < 1$. As a result, for fixed $\omega R < 1$ the length of the plateau in $\log\theta$ is $-\log(\omega R)$ while it disappears completely for $\omega R > 1$. This is the reason why the spectrum in ω shown in Fig. 3 shows two very distinct regimes.

(i) $\omega R \ll 1$. In this regime the amplitude (13) is well approximated by dropping the log term in $\Phi(z)$ [except if $|\boldsymbol{bq}| \gg 1$, in which case, owing to $\Phi(z) \to z^2$ as $z \to 0$, the amplitude behaves as $\sim 1/|\boldsymbol{bq}|^2$ (Fig. 2)]. Using the representation (6) and the soft approximation for $\mathfrak{M}$, we obtain the frequency distribution integrated over the whole solid angle:

$$\frac{dE^{\mathrm{GW}}}{d\omega} = \frac{Gs}{\pi}\boldsymbol{\theta}_s^2 \int_0^1 \frac{2\theta d\theta}{\sqrt{1-\theta^2}} \frac{d\phi}{\pi} \frac{\sin^2\phi_q}{|\boldsymbol{\theta}-\boldsymbol{\theta}_s|^2} \Theta\left(\frac{1}{b\omega} - \theta\right)$$
$$\simeq \frac{Gs}{\pi}\boldsymbol{\theta}_s^2 \left[2\log\ \min\left(\frac{b}{R}, \frac{1}{\omega R}\right) + \mathrm{const}\right]. \tag{16}$$

We see that the really infrared regime holds only in the tiny region $\omega < 1/b$, with a rapidity plateau up to $|y| < Y_s \equiv \log(b/R)$ (Fig. 2), much smaller than $Y = \log(Eb/\hbar)$, the rapidity available in the single H diagram emission. On the other hand, here the small-ω number density in rapidity, $(Gs/\pi)\boldsymbol{\theta}_s^2$, agrees with the one used in Ref. [9] and with the zero-frequency limit (ZFL) of Refs. [19,20].

(ii) $1 < \omega R < \omega_M R$. In this region the two terms of $\Phi(z)$ are of the same order, but for $\omega R \gtrsim 1$ we can look at the integrated distribution by reliable use of the completeness of the $\boldsymbol{q}$ states and we obtain ($\omega R \gtrsim 1$)

$$\frac{dE^{\mathrm{GW}}}{d\omega} = \frac{2Gs\boldsymbol{\theta}_s^2}{\pi^2} \int \frac{d^2z}{|z|^4} |\Phi(z)|^2 \left(\frac{\sin\omega Rx}{\omega Rx}\right)^2. \tag{17}$$

The spectrum (17) decreases like $1/(\omega R)^2$ for any fixed value of x, in front of an integral which is linearly divergent for $x \to 0$. This means effectively a $1/(\omega R)$ energy-emission spectrum [17], whose origin is the decoherence effect induced by $\omega R > 1$ on the graviton emission along the eikonal chain. Furthermore, modulo an overall factor $\boldsymbol{\theta}_s^2$, the shape of the spectrum is universal above $\omega \simeq b^{-1}$ and tuned on R^{-1} (blue curve in Fig. 3).

Thus, the total emitted energy fraction is small, of order $\boldsymbol{\theta}_s^2$, and, to logarithmic accuracy:

$$\frac{E^{\mathrm{GW}}}{\sqrt{s}} \sim \frac{2}{3}\log(e/2)\boldsymbol{\theta}_s^2(\boldsymbol{b})\log(\omega_M R), \tag{18}$$

where ω_M is an upper frequency cutoff.

Quantum mechanically ω_M cannot exceed $E/\hbar$, but we expect that the classical theory ($\hbar \to 0$) should provide by itself a cutoff. It was argued in Ref. [15] that it should correspond to an emission rate $dE^{\mathrm{GW}}/dt \sim G_N^{-1}$ (sometimes referred to as the Dyson bound) in which a Planck energy is emitted per Planck time or, classically, the emitted energy does not have enough time to get out of its own Schwarzschild radius. For our spectrum falling like ω^{-1}, this gives $R\omega < \boldsymbol{\theta}_s^{-2}$ and, consequently, a total fraction of energy loss of order $\boldsymbol{\theta}_s^2 \log \boldsymbol{\theta}_s^{-2}$, neatly resolving the "energy crisis."

A final question, which deserves attention, is whether we can actually calculate correlated emission also, by describing the situation in which neighboring exchanges act coherently, or a single exchange emits many gravitons. The latter correlations originate from multi-H diagrams [10] and thus contain higher powers of R^2/b^2 in the eikonal, the former ones have been investigated as rescattering corrections [11]. They may give rise to higher powers of Φ and perhaps to the exponentiation proposed in Ref. [15] and to a classical large-ω cutoff, but further investigation is needed in order to confirm such a guess.

To summarize, we have shown that the spectrum of graviton emission in trans-Planckian collisions takes a simple and elegant limiting form, which unifies the soft and Regge behaviors of the S matrix, and is determined by the spin-2 structure of the interaction. At low enough energy the spectrum reproduces the expected (finite) ZFL. But its shape above $\omega \sim b^{-1}$ is universal and tuned on R^{-1}, deviating from the ZFL by a power of ω above $\omega \sim R^{-1}$, in agreement with recent classical results [15,16]. Because of the role of R^{-1}, the characteristic frequency or energy of the emitted gravitons *decreases* when the energy of the collision is *increased* above the Planck scale.

At small deflection angles the radiation is still concentrated around two cones of size $\mathcal{O}(\boldsymbol{\theta}_s)$ around the colliding particles, with energies up to $\mathcal{O}(R^{-1})$ and transverse momenta $\mathcal{O}(b^{-1})$. Extrapolating qualitatively the spectrum till $b \sim R$, where classical gravitational collapse is expected to occur, suggests a smooth quantum transition between the dispersive and collapsing regimes in trans-Planckian energy collisions. Such a smooth transition was already argued to occur in the string-dominated regime [21] and, more recently, in a $2 \to N$ high-energy, high-multiplicity annihilation process integrated over $\boldsymbol{b}$ [22].

We are grateful to Francesco Coradeschi for several useful discussions. We also wish to thank the Galileo Galilei Institute for Theoretical Physics and the Kavli Institute for Theoretical Physics, University of California, Santa Barbara (research supported in part by the National Science Foundation under Grant No. NSF PHY11-25915).

---

*ciafaloni@fi.infn.it
†colferai@fi.infn.it
‡gabriele.veneziano@cern.ch

[1] M. Duff, Phys. Rev. D **7**, 2317 (1973).
[2] D. Amati, M. Ciafaloni, and G. Veneziano, Phys. Lett. B **197**, 81 (1987).
[3] D. Amati, M. Ciafaloni, and G. Veneziano, Int. J. Mod. Phys. A **03**, 1615 (1988).
[4] D. Amati, M. Ciafaloni, and G. Veneziano, Phys. Lett. B **216**, 41 (1989).
[5] D. J. Gross and P. F. Mende, Phys. Lett. B **197**, 129 (1987).
[6] D. J. Gross and P. F. Mende, Nucl. Phys. **B303**, 407 (1988).
[7] P. Aichelburg and R. Sexl, Gen. Relativ. Gravit. **2**, 303 (1971).
[8] S. B. Giddings, Phys. Rev. D **74**, 106006 (2006).
[9] D. Amati, M. Ciafaloni, and G. Veneziano, Nucl. Phys. **B347**, 550 (1990).
[10] D. Amati, M. Ciafaloni, and G. Veneziano, J. High Energy Phys. 02 (2008) 049.
[11] M. Ciafaloni and D. Colferai, J. High Energy Phys. 10 (2014) 85.
[12] X. O. Camanho, J. D. Edelstein, J. Maldacena, and A. Zhiboedov, arXiv:1407.5597.
[13] G. D'Appollonio, P. Di Vecchia, R. Russo, and G. Veneziano, J. High Energy Phys. 05 (2015) 144.
[14] V. S. Rychkov (private communication).
[15] A. Gruzinov and G. Veneziano, arXiv:1409.4555.
[16] P. Spirin and T. N. Tomaras, J. High Energy Phys. 06 (2015) 153.
[17] M. Ciafaloni, D. Colferai, F. Coradeschi, and G. Veneziano (to be published).
[18] L. N. Lipatov, Zh. Eksp.Teor. Fiz. **82**, 991 (1982) [Sov. Phys. JETP **55**, 582 (1982)].
[19] S. Weinberg, Phys. Rev. **140**, B516 (1965).
[20] L. Smarr, Phys. Rev. D **15**, 2069 (1977).
[21] G. Veneziano, J. High Energy Phys. 11 (2004) 001.
[22] G. Dvali, C. Gomez, R. Isermann, D. Lüst, and S. Stieberger, Nucl. Phys. **B893**, 187 (2015).